When Does the Uncertainty Become Non-Gaussian

Kyle T. Alfriend[1]
Texas A&M University
Inkwan Park[2]
Texas A&M University

ABSTRACT

The orbit state covariance is used in the conjunction assessment/probability of collision calculation. It can also be a valuable tool in track association, maneuver detection and sensor tasking. These uses all assume that the uncertainty is Gaussian. Studies have shown that the uncertainty at epoch (time of last observation) is reasonably Gaussian, but the neglected nonlinearities in the covariance propagation eventually result in the uncertainty becoming non-Gaussian. Numerical studies have shown that for space objects in low Earth orbit the covariance remains Gaussian the longest in orbital element space. It has been shown that the covariance remains Gaussian for up to 10 days in orbital element space, but becomes non-Gaussian after 2-3 days in Cartesian coordinates for a typical LEO orbit. The fundamental question is when does it become non-Gaussian and how can one given the orbit state and covariance at epoch determine when it occurs. A tool that an operator could use to compute the approximate time when the when the uncertainty becomes non-Gaussian would be useful This paper addresses the development of such a tool.

1. INTRODUCTION

The orbit covariance of a space object is, or can be used, in the important space situational awareness (SSA) processes including a) conjunction assessment and probability of collision [1,2], b) uncorrelated track (UCT) association [3], maneuver detection [4], and d) sensor tasking [5]. To make the correct decision requires that the covariance represent the actual uncertainty. Figure 1 shows the impact of the size of the covariance being incorrect. In this example the probability of collision is computed for a typical example and then the size of the covariance is increased, the abscissa is the multiplicative factor of the covariance. Note a factor of two increase in the size of the covariance (K=2), the probability of collision increases more than three orders of magnitude, and this is in the range where the decision to maneuver is made, P_C=0.0001-0.001. This illustrates the necessity in having a realistic uncertainty.

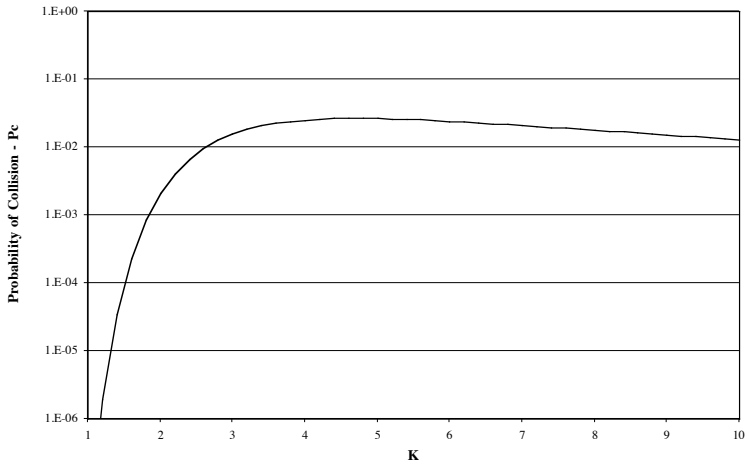

Figure 1 Probability of Collision vs Covariance Size

[1] TEES Distinguished Research Professor of Aerospace Engineering
[2] Postdoctoral Research Associate

All of these processes currently assume that the uncertainty is Gaussian. The propagation is propagated according to

$$P(t) = \Phi(t,t_0) P(t_0) \Phi^T(t,t_0) \tag{1}$$

where $\Phi(t,t_0)$ is the state transition matrix of the 1st variational equations. Thus, the, propagation is based on linear equations. The neglected nonlinearities in this propagation cause the initial Gaussian uncertainty to become non-Gaussian. Junkins [6] showed that the propagation stays linear the longest on orbital element space and the shortest in Cartesian space. Sabol showed that for space objects in LEO in catalog maintenance and not perturbed by atmospheric drag that the covariance stays Gaussian for up to 10 days, whereas in Cartesian elements it becomes non-Gaussian in 2-3 days. The metric used by Sabol was the Mahalanobis distance, but the decision on when the covariance becomes non-Gaussian was qualitative, not quantitative.

The primary nonlinearity that causes the uncertainty to become non-Gaussian is the error in the semi-major axis. This error causes secular growth in the in-track direction, that is an error in the mean and true anomaly. Secular growth in the out of plane direction is primarily caused by an inclination error, but this secular growth is proportional to the equatorial bulge term, $J_2 = 0.00108,$ which means it should be much smaller than the in-track secular growth. This paper addresses the problem of determining when the orbit uncertainty becomes non-Gaussian. The key questions addressed here are

1. What metric should be used to determine when the uncertainty is non-Gaussian?
2. Since the secular in-track error growth is due primarily to the semi-major axis error can the 2D semi-major axis-mean anomaly space be used to determine when the uncertainty becomes Gaussian?
3. Can an analytic result be obtained to estimate when the uncertainty becomes non-Gaussian? If so, this would be a very useful tool.

2. CRAMER VON MISES METRIC

The metric for determining when the uncertainty becomes non-Gaussian is the Cramer von Mises (CVM)metric suggested by Horwood, et. al. [7]. Drummond, et. al. [8] calls this metric a track consistency measure and it uses the Mahalanobis distance [9]. Key properties of the metric include

- It can be used with any coordinate system used to represent the uncertainty.
- It includes each component of the state.
- It is dimensionless.
- It is computationally rigorous and statistically rigorous.

In addition to these properties the CVM can be used with a closed form cumulative distribution function (cdf) or when the results are numerical from a Monte Carlo. The Mahalanobis distance is defined by

$$MD = k^2 = \left(\mathbf{x} - \mathbf{x}_{truth}\right)^T P^{-1} \left(\mathbf{x} - \mathbf{x}_{truth}\right) \tag{2}$$

where **x** is the state and *P* is the covariance. The quantity *k* is the number of standard deviations. For a conservative linear system the MD is constant along a trajectory. The CVM when the uncertainty (pdf) has an analytic representation is

$$\omega^2 = \int_0^{k_m} \left[F_n(k) - F^*(k)\right]^2 dF^* \tag{3}$$

where $F^*(k)$ is the cdf of the Mahalanobis distance and $F_n(k)$ is the approximate cdf of the MD representing the *n* degree of freedom system being analyzed. For a two degree of freedom system

$$F^*(k) = 1 - \exp\left(-0.5k^2\right) \tag{4}$$

which results in

$$\omega^2 = \int_0^{k_m} \left[F_n(k) - F^*(k)\right]^2 k \exp\left(-0.5k^2\right) dk \tag{5}$$

When the results are from a Monte Carlo with *m* samples the CVM is

$$\omega^2 = \frac{1}{12m} + \sum_{i=1}^{m} \left[\frac{2i-1}{2m} - F\left(x_i\right)\right] \tag{6}$$

Horwood, et. al. also discuss and evaluate the Anderson-Darling [10] metric which we also use for comparison. Table 1 shows the range of the CVM metric as a function of the confidence factor $\left(1-\alpha\right)$. For example if $\omega^2 < 1.16204$ there is a 99.9% probability that the uncertainty is Gaussian. From Eq. (5) it is obvious that if the uncertainty is Gaussian with the same standard deviation $\omega^2 = 0$.

Table 1 CVM Metric Range as a function of the Confidence Level

Sample size	$1-\alpha$			
∞	90%	95%	99%	99.9%
	[0,0.34730]	[0,0.46136]	[0.0.74346]	[0,1.16204]

3. THE SEMI-MAJOR AXIS-MEAN ANOMALY SYSTEM

The equations of motion for the 2D semi-major axis-mean anomaly space are

$$\begin{aligned} &\dot{a} = 0, a = a_0 \\ &\dot{l} = n = \sqrt{\frac{\mu}{a^3}}, l = nt + l_0 \end{aligned} \tag{7}$$

Let $\left(\hat{a}, \hat{l}\right)$ be the estimated state, let $\tau = \hat{n}t$ and expand about this state. This gives

$$\begin{aligned} &a = \hat{a} + \delta a \\ &l = \hat{l} + \delta l \\ &\delta\overline{a} = \delta a / \hat{a} \\ &\frac{d}{d\tau}(\ ) = (\ )' \\ &\delta\overline{a}' = 0, \delta\overline{a} = \delta\overline{a}_0 \\ &\delta l = \left[\left(1+\delta\overline{a}\right)^{-3/2} - 1\right]\tau + \delta l_0 \approx \left(-\frac{3}{2}\delta\overline{a} + \frac{15}{8}\delta\overline{a}^2\right)\tau + \delta l_0 \end{aligned} \tag{8}$$

With $\mathbf{x} = \left(\delta\overline{a}, \delta l\right)^T$ the solution is

$$\mathbf{x}(\tau) = \Phi(\tau)\mathbf{x}_0 + \mathbf{x}_{NL}$$
$$\Phi(\tau) = \begin{pmatrix} 0 & 0 \\ -1.5\tau & 1 \end{pmatrix}, \mathbf{x}_{NL} = \begin{pmatrix} 0 \\ \frac{15}{8}\delta\bar{a}^2\tau \end{pmatrix} \tag{9}$$

The covariance propagates according to

$$P(\tau) = \Phi P_0 \Phi^T$$
$$P_0 = \begin{pmatrix} \sigma_{\delta\bar{a}}^2 & \rho\sigma_{\delta\bar{a}}\sigma_{\delta l_0} \\ \rho\sigma_{\delta\bar{a}}\sigma_{\delta l_0} & \sigma_{\delta l_0}^2 \end{pmatrix} \tag{10}$$

The Mahalanobis becomes

$$k^2 = k_0^2 + \left(\frac{225}{64}\right)\left[\frac{\delta\bar{a}^4}{\sigma_{\delta l_0}^2\left(1-\rho^2\right)}\right]\tau^2 + \left(\frac{15\delta\bar{a}^2}{4}\right)\left[\frac{\left(\sigma_{\delta\bar{a}}^2\delta l_0 - \rho\sigma_{\delta\bar{a}}\sigma_{\delta l_0}\right)\delta\bar{a}}{\sigma_{\delta\bar{a}}^2\sigma_{\delta l_0}^2\left(1-\rho^2\right)}\right]\tau \tag{11}$$

Now let $\rho = 0$ and

$$y_1 = \frac{\delta\bar{a}}{\sigma_{\delta\bar{a}}} = r\cos\theta$$
$$y_2 = \frac{\delta l_0}{\sigma_{\delta l_0}} = r\sin\theta \tag{12}$$

Eq. (11) becomes

$$k^2 = r^2 + \left(\frac{225}{64}\right)\left(\frac{\sigma_{\delta\bar{a}}^4\tau^2 r^4}{\sigma_{\delta l_0}^2}\right)\cos^4\theta + \left(\frac{15}{4}\right)\left(\frac{\sigma_{\delta\bar{a}}^2 r^3\tau}{\sigma_{\delta l_0}}\right)\cos^2\theta\sin\theta \tag{13}$$

Figure 2 shows the result from a Monte Carlo of simulation of the exact equations of motion with standard deviations of $a = 7000\ km, \sigma_{\delta a} = 5\ km$ and $\sigma_{\delta l_0} = 1/a$. The boundaries are plotted using Eq. (13) for k=1. The points are those for k<1 from the exact solution. Since the points are all contained within the k=1 curve it can be concluded that the approximate solution of the mean anomaly given by Eq. (8) captures the necessary nonlinear effects. Figure 3 shows curves of constant k for $a = 7000\ km, \sigma_{\delta a} = 5\ km$ and $\sigma_{\delta l_0} = 1/a$. Even after one orbit the deviation from the Gaussian ellipsoid is obvious.

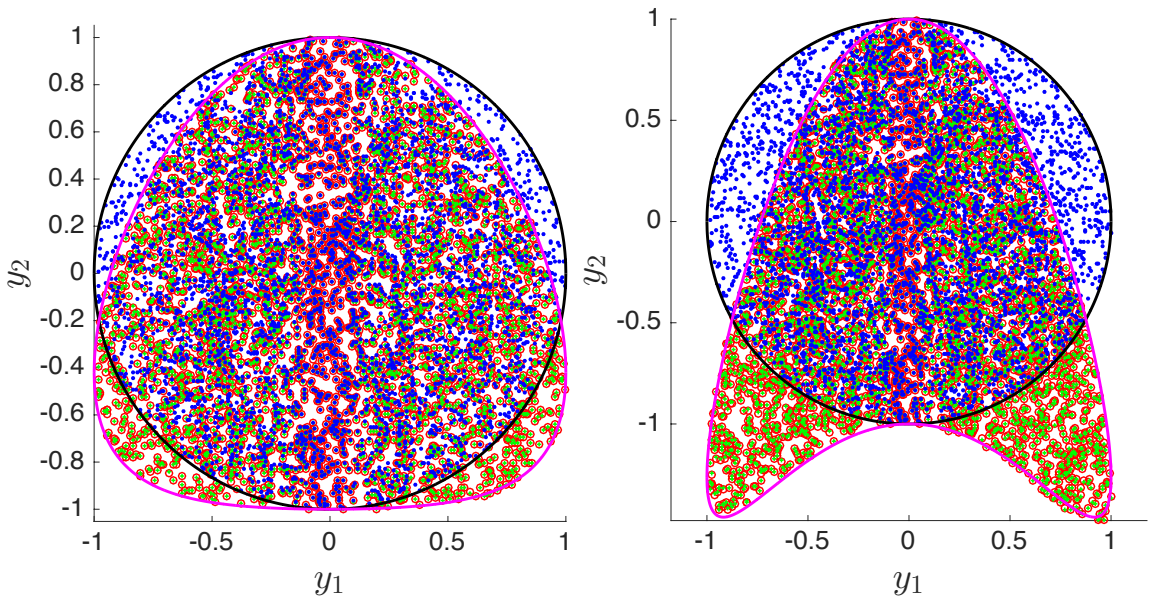

Figure 2 Simulation Results Comparing Exact and Approximate Solutions for *k*=1 for 10 and 30 Orbits

Figure 3 shows curves of constant k for $a = 7000\ km, \sigma_{\delta a} = 5\ km$ and $\sigma_{\delta l_0} = 1/a$. These are not covariance plots as the axes are related to the initial state, not current state. As evident from Eq. (13) without the nonlinear effects the curve remains a circle. The distortion from the initial Gaussian distribution is evident after five orbits. Later results will show that the uncertainty becomes non-Gaussian after 5.7 orbits.

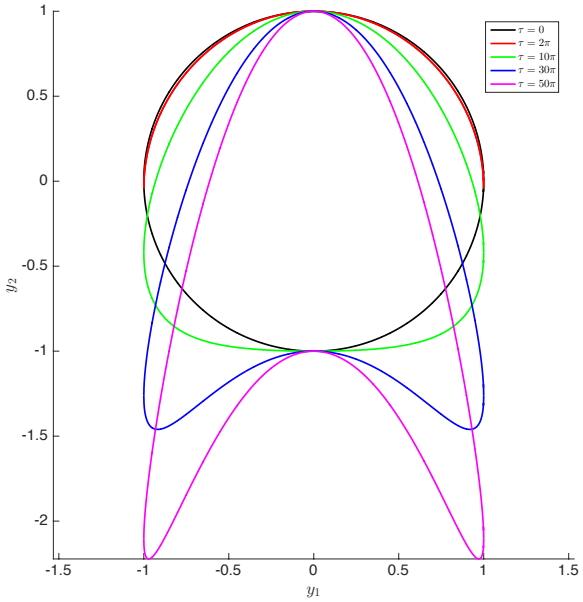

Figure 3 Constant *k* Curves for 0, 1, 5, 15, 25 orbits

Figure 4 compares the CVM and Anderson-Darling metric for determining the time when the uncertainty becomes non-Gaussian with 99.9% confidence for the initial conditions $\left(a = 7000km, \delta a = 5km, \delta l_0 = 1/a, \sigma_{\delta l_0} = 1/a\right)$ as a function of the semi-major axis standard deviation. These results were obtained using the numerical form for the metric, Eq. (6).with 10,000 samples. The results show that both metrics give the same answer. Figure 5 shows the effect of various values of the initial in-track error standard deviation. The time for the uncertainty to become non-Gaussian increases as the initial in-track error standard deviation increases.

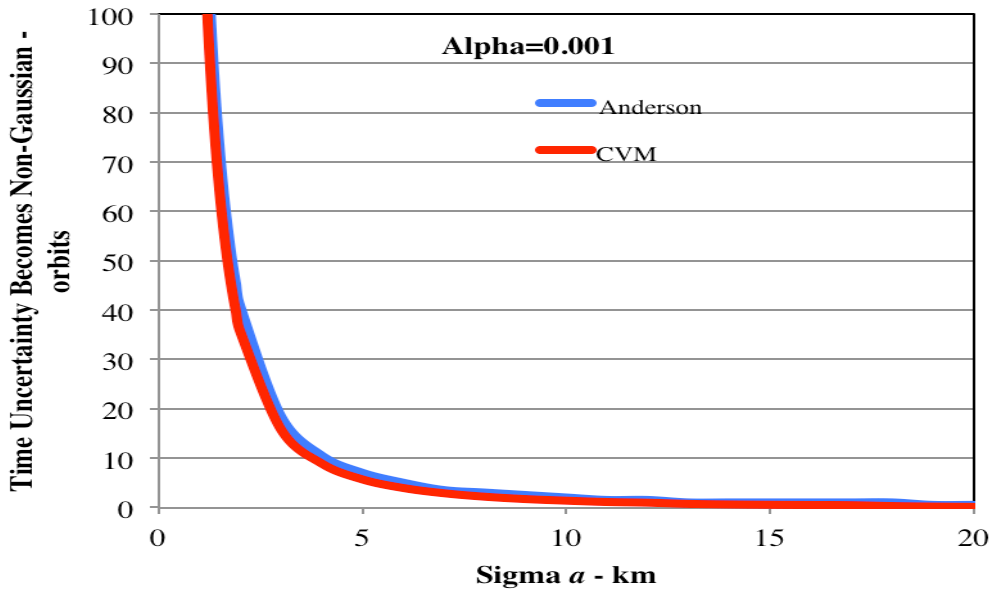

Figure 4 Comparion of the Cramer von Mises and Anderson-Darling Metrics for the 2D Case

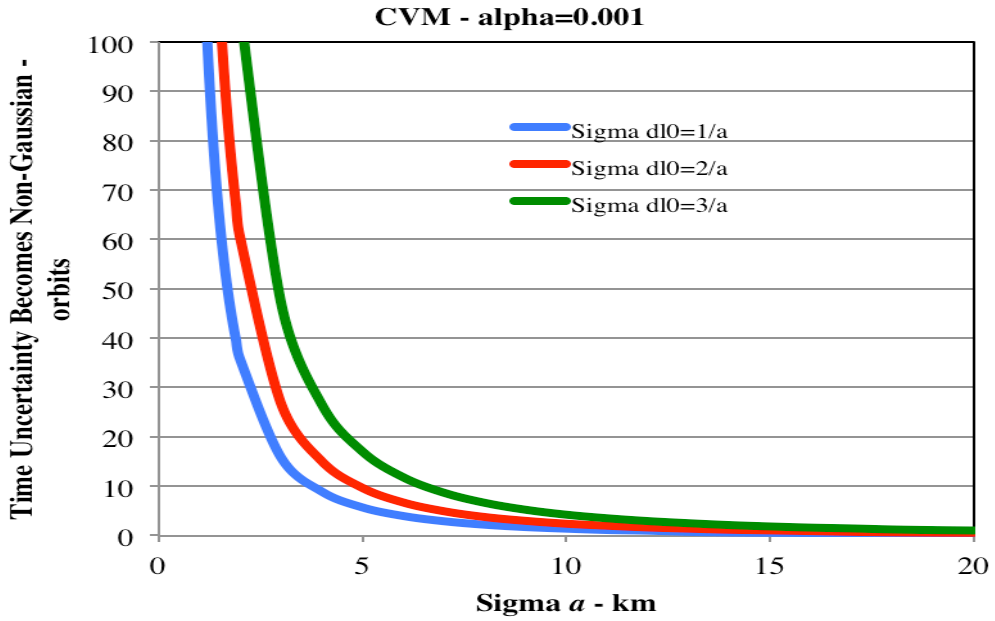

Figure 5 Time Uncertainty Becomes Non-Gaussian For Various Initial In-Track Standard Deviations

4. 6D-2D COMPARISON

The question can the analysis of the semi-major axis-mean anomaly space determine when the uncertainty in the real world 6D orbital element case become non-Gaussian is now addressed. The parameters used in the analysis were:

$$
\begin{aligned}
&2D \\
&a = 7000km, \sigma_{\delta a} \text{ varied} \\
&l_0 = 0, \sigma_{\delta l_0} = 1/a \\
&6D \\
&a = 7000km, \sigma_{\delta a} \text{ varied} \\
&l_0 = 105, \sigma_{\delta l_0} = 1/a \\
&e = 0.001, \sigma_e = 0.0001 \\
&i = 51.6\deg, \sigma_i = 0.5/a \\
&\omega = 194, \sigma_\omega = 0.5/a \\
&\Omega = 220, \sigma_\Omega = 0.5/a
\end{aligned}
\tag{14}
$$

There was no correlation between any of the parameters. The initial conditions were obtained in the usual manner with a random number generator and 10,000 samples were generated. Figure 6 compares the time for the uncertainty to become non-Gaussian for the 2D and 6D orbital element spaces. The 2D estimate is slightly conservative. The results clearly show the 2D semi-major axis-mean anomaly element space can be used to estimate when the 6D uncertainty will become non-Gaussian. We have not yet investigated cases that do not have a small eccentricity.

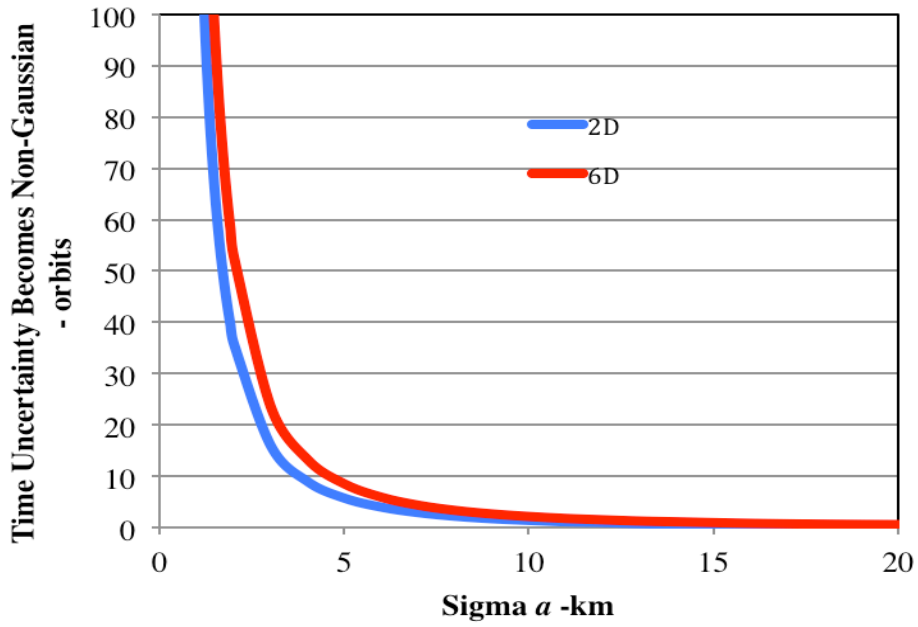

Figure 6 Comparison of the 2D and 6D Orbital Element Formulations

Using the same initial conditions the 6D Cartesian coordinate uncertainty was investigated. The Cartesian state was computed by transforming the orbital elemts for each sample to Cartesian coordinates and the initial covariance was determined in the usual manner with the Jacobian. Figure 7 compares the 6D case for orbital elemnts and Cartesian coordinates. For small $\sigma_{\delta a}$ the uncertainty becomes non-Gaussian much sooner, but for large $\sigma_{\delta a}$ the two times are

essentially equal. This is due to the fact the the uncertainty in orbital element space at epoch is assumed to be Gaussian, but the transformation to Cartesian space results in an uncertainty that is not Gaussian at epoch, but it has not yet crossed the non-Gaussian threshold for the CVM metric.

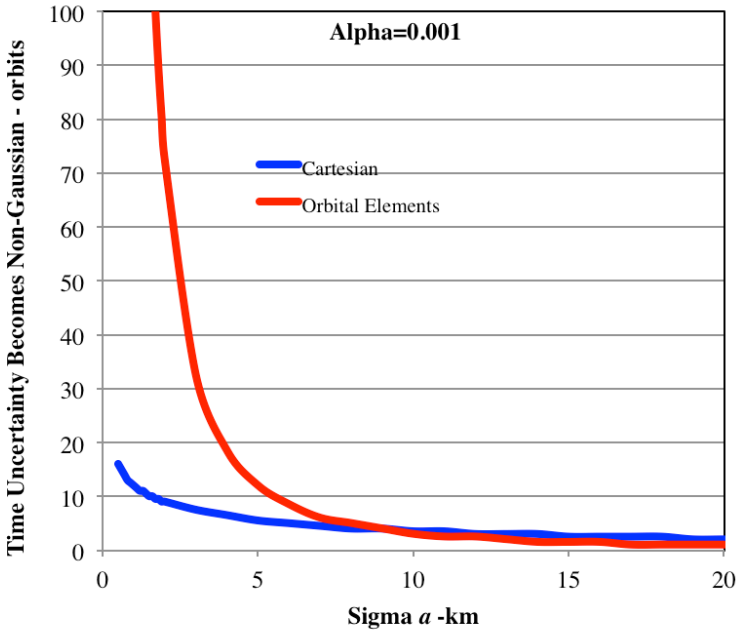

Figure 7 Comparison of the 6D Cartesian and Orbital Element Spaces

5. 2D ANALYTIC APPROACH

The CVM metric Eq. (5) is

$$\omega^2 = \int_0^{k_m} \left[F_n(k) - F^*(k) \right]^2 k \exp\left(-0.5k^2\right) dk$$
$$F^*(k) = 1 - \exp\left(-0.5k^2\right) \tag{15}$$

where $F^*(k)$ is the cumulative distribution function (cdf) of the Gaussian Mahalanobis distance and $F(k)$ is the approximate cdf of the system equations, Eq. (9). Given the transformation $z = g(\mathbf{x})$ the cdf of z is given by

$$F(z) = \int_D f(\mathbf{x}) d\mathbf{x} \tag{16}$$

where the region D is defined by $z < g(\mathbf{x})$. Applying this to the Mahalanobis distance gives

$$F(k) = \int_D f(\mathbf{x}_0) d\mathbf{x}_0 = \frac{1}{2\pi\sigma_{\delta\bar{a}}\sigma_{\delta l_0}} \int_D \exp\left(-0.5\mathbf{x}_0 P^{-1} \mathbf{x}_0\right) d\mathbf{x}_0$$
$$F(k) = \frac{1}{2\pi} \int_D r \exp\left(-0.5r^2\right) dr d\theta \tag{17}$$

where D is defined by

$$k^2 < r^2 + \left(\frac{225}{64}\right)\left(\frac{\sigma_{\delta\bar{a}}^4 \tau^2 r^4}{\sigma_{\delta l_0}^2}\right)\cos^4\theta + \left(\frac{15}{4}\right)\left(\frac{\sigma_{\delta\bar{a}}^2 r^3 \tau}{\sigma_{\delta l_0}}\right)\cos^2\theta\sin\theta \tag{18}$$

In Eq. (18) for now it has been assumed $\rho = 0$. When the nonlinearities are neglected the region D is defined by $k < r$ and Eq. (17) becomes

$$F(k) = \frac{1}{2\pi}\int_0^k \int_0^{2\pi} r\exp\left(-0.5r^2\right) dr d\theta = 1 - \exp\left(-0.5k^2\right) \tag{19}$$

When the nonlinear effects are included the issue is how to incorporate the constraint of Eq. (18) into the limits of integration of θ. To date the solution has not been found.

6. SUMMARY

The research questions addressed in this paper are:

1. What metric should be used to determine when the uncertainty is non-Gaussian?
2. Since the secular in-track error growth is due primarily to the semi-major axis error can the 2D semi-major axis-mean anomaly space be used to determine when the uncertainty becomes Gaussian?
3. Can an analytic result be obtained to estimate when the uncertainty becomes non-Gaussian? If so, this would be a very useful tool.

Due to key properties of the Cramer von Mises metric it was selected for the metric for measuring when the uncertainty becomes non-Gaussian. It uses the Mahalanobis distance and a key reason it was selected is that it has an analytic form that uses an analytic representation of cumulative distribution function for the Mahalanobis distance that is needed for Question 3. The answer to Question 2 is YES, at least for objects of low eccentricity. This opens up a good opportunity for making the analysis of the 6D case simpler. Question 3 has not yet been answered. It requires an analytic representation of the cumulative distribution function of the Mahalanobis distance and this is challenging.

7. REFERENCES

1. Foster, J., "A Parametric Analysis of Orbital Debris Collision Probability and ManeuverRateforSpaceVehicles,"NASAJSC-25898,European Space Agency, Aug. 1992.
2. Akella, M.R. and Alfriend, K.T., "The Probability of Collision Between Space Objects", *AIAA Journal of Guidance, Control and Dynamics,* Vol. 23, No. 5, pp. 769-772, September 2000.
3. Hill, K., Sabol, C. and Alfriend, K.T., "Comparison of Covariance-Based Track Association Approaches With Simulated Radar Data," *AAS J. of the Astronautical Sciences*, Vol. 59, Nos. 1 & 2, Jan-June 2012, pp. 287-306.
4. Holzinger, M.J., Scheeres, D.J. and Alfriend, K.T., "Object Correlation, Maneuver Detection, and Characterization Using Control Distance Metrics with Uncertain Systems," *AIAA J. of Guidance, Control and Dynamics*, Vol. 35, No. 4, July-August 2012, pp. 1312-1325.
5. Hill, K, Sydney, P., Hamada, K. Cortez, R., Luu, K.K., Schumacher, P.W. and Jah, M., "Covariance Based Scheduling of a Network of Optical Sensors, " Paper No. AAS 10-325, 2010 Space Flight Mechanics Conference, Kyle T. Alfriend Astrodynamics Symposium, Monterey, CA, May 2010.
6. Junkins, J.L., Akella, M.R., Alfriend, K.T., "Non-Gaussian Error Propagation in Orbital Mechanics," *AAS Journal of Astronautical Sciences,* Vol. 44, No. 4, Oct.-Dec. 1996, pp. 541-563.

7. Horwood, J.T, Aristoff, J.M., Singh, N., Poore, A.B. and Hejduk, M.D. “Beyond Covariance Realism: A New Metric for Uncertainty Realism”, SPIE Proceedings: Signal and Data Processing of Small Targets, 2014, Vol. 9092.
8. Drummond, O. E., Ogle, T. L., and Waugh, S., “Metrics for Evaluating Track Covariance Consistency,” in [SPIE Proceedings: Signal and Data Processing of Small Targets 2007], 6699 (2007).
9. Mahalanobis, P. C., “On the generalised distance in statistics,” Proceedings of the National Institute of Sciences of India 2(1), 49–55 (1936)
10. Anderson, L.W. and Darling, D.A., “Asymptotic Theory of Certain "Goodness of Fit" Criteria Based on Stochastic Processes,” *The Annals of Mathematical Statistics,* Vol. 23, No. 2, pp193-212.